On the seasonal asymmetry of the diurnal and semidiurnal geomagnetic variations

A. Chulliat, E. Blanter, J. -L. Le Mouël, M. Shnirman

On the seasonal asymmetry of the diurnal and semidiurnal geomagnetic variations

A. Chulliat,[1] E. Blanter,[2] J.-L. Le Mouël,[1] and M. Shnirman[2]

Received 20 April 2004; revised 14 January 2005; accepted 28 January 2005; published 4 May 2005.

[1] The diurnal and semidiurnal variations of the geomagnetic field are investigated at 18 observatories using long series of hourly values (up to 97 years at Sitka). The seasonal variations of amplitude of the 12-hour and 24-hour lines are obtained for the *H* and *Z* components using a 28-day sliding window. The Fourier analysis is performed using either all days within the window or only the five quietest days. At midlatitudes a strong lack of symmetry about the summer solstice is observed for both lines and both components. This effect is enhanced when selecting quiet days. When averaged over the entire series, the sign of this seasonal asymmetry is the same at 9 out of 10 midlatitude observatories for both lines and for a given component; it is opposite for the *H* and *Z* components. Such a coherent seasonal asymmetry is not found at low and high latitudes. At high latitudes a strong annual variation is found inside the polar caps, while a strong semiannual variation is found in the auroral zones. When selecting quiet days, these two effects are weaker, and the seasonal asymmetry becomes comparable to that at midlatitudes. At all latitudes the year-to-year variations of the seasonal asymmetry are uncorrelated with solar activity. It is suggested that lower thermospheric winds may have a similar seasonal asymmetry between spring and autumn equinoxes. Such an asymmetry is present in the published literature but has been overlooked. Possible causes for this wind asymmetry are reviewed.

Citation: Chulliat, A., E. Blanter, J.-L. Le Mouël, and M. Shnirman (2005), On the seasonal asymmetry of the diurnal and semidiurnal geomagnetic variations, *J. Geophys. Res.*, *110*, A05301, doi:10.1029/2004JA010551.

1. Introduction

[2] The discovery of the geomagnetic daily variation is attributed to Graham in 1724. A thorough description of this variation was made by Arago, who performed 50,000 measurements from 1820 to 1835. Since these pioneering works, a lot of studies have been devoted to the daily variation. It has been established that the daily variation during quiet solar conditions is mostly generated by winds in the lower thermosphere flowing through the Earth's main magnetic field, a process known as the ionospheric wind dynamo [*Chapman*, 1929; *Richmond et al.*, 1976]. Its main Fourier components are the 24-hour line and its harmonics (12, 8, and 6 hours, etc.) which are produced by solar tides and often referred to as S_q (''solar quiet day'') variations, and the 12 h 25 min line and a few other detectable lines produced by lunar tides, which are often referred to as *L* (''lunar'') variations. The main features of the various components of the daily variations have been reasonably well described, in particular, by spherical harmonic models of equivalent current systems in the ionosphere [*Chapman and Bartels*, 1962; *Campbell*, 1989].

[3] Following *Lloyd* [1874], it used to be customary in early studies of the daily variation to subdivide the year into three seasons: southern summer (November, December, January, February), equinox (March, April, September, October), and northern summer (May, June, July, August). That is, it was implicitly assumed that the daily variation is a function of the Sun's declination, so that spring and autumn equinoxes are symmetrical from a geomagnetic point of view. However, as soon as long series of observatory data were made available, it appeared that Lloyd's grouping is too simplistic and that the daily variation varies with season in a more complicated way [*Howe*, 1950].

[4] *Wulf* [1963, 1965a, 1965b] investigated this symmetry breaking in a systematic way at three midlatitude observatories: Honolulu, Tucson, and San Juan (Puerto Rico). Using hourly values from five quiet days of each month, he computed the monthly averages of the daily range of the variation of the horizontal (*H*) component over a full solar cycle (1948–1958) at each observatory, and over the interval 1917–1936 at Honolulu. Each time *Wulf* [1963, p. 525] found that ''there are differences of range and of form in the daily variation that do not follow solar declination in a simple way.'' Specifically, he found that the range in March is larger than that in September in Honolulu and San Juan, but smaller in Tucson. He reviewed several possible causes for this observation and, having dismissed

[1]Laboratoire de Géomagnétisme, Institut de Physique du Globe de Paris, Paris, France.
[2]International Institute of Earthquake Prediction Theory and Mathematical Geophysics, Moscow, Russia.

0148-0227/05/2004JA010551

ionospheric conductivity, main geomagnetic field, induction and geomagnetic activity, he concluded that the most plausible cause was an anomalous seasonal variation of the lower ionosphere large-scale air circulation.

[5] Despite Wulf's enthusiastic statement that "there is an unusual opportunity here to extend the scope of meteorological research" [*Wulf*, 1963], very few studies were subsequently devoted to the seasonal asymmetry of the S_q variations. The much stronger seasonal asymmetry in the lunar variations apparently drew more attention [*Stening and Winch*, 1979; *Schlapp and Malin*, 1979; *Gupta*, 1982]. A tentative explanation for the asymmetry of the S_q variations was proposed by *Campbell and Matsushita* [1982, p. 5308]: "At midlatitudes the summertime appearance of the *Sq* range maximum, about a month and a half after the June solstice, shows the dependence of the ionospheric dynamo current upon the atmospheric *E* region wind strength and pattern which seem therefore to have a seasonal symmetry that lags the solstice by a duration equivalent to that found for tropospheric heating." This observation was based on a spherical harmonic analysis of the S_q field in the North American sector in 1965. *Campbell and Schiffmacher* [1985] later found an asymmetry of opposite sign in the European sector in the same year. *Campbell and Schiffmacher* [1985, p. 6485] concluded that "it may be possible that the spring heating of the atmosphere along the eastern Atlantic coast by the Gulf Stream (together with the semiannual modulation) couples, in some way, to the upper atmosphere and moves the maximum in thermotidal ionospheric motion from the expected summer solstice back to May." More recently, *Takeda* [2002] analyzed the global S_q field each year from 1980 to 1990 and found different morphologies of the equivalent current system in March and September. He attributed this effect to a similar asymmetry in tidal winds in the upper atmosphere. However, unlike Wulf's study, none of these studies are based on data sets longer than one solar cycle.

[6] Our goal in the present paper is to revisit the problem of the seasonal asymmetry of the geomagnetic daily variations produced by solar tides, using modern magnetic data and putting the results in the context of recent advances in our understanding of the ionospheric wind dynamo. Thanks to the advent of a global network of high-quality geomagnetic observatories, as well as modern computing and storage facilities, long series of homogeneous geomagnetic data are now easily available and processable. Compared to Wulf's time, 40 more years of data are now available, at many more observatories. Numerical simulations of the ionospheric wind dynamo combined with magnetic observations have provided a lot of information about the mutual coupling between ionospheric currents and lower thermospheric winds [*Richmond*, 1989, 1995]. In parallel, important progress has been made in our understanding of the dynamics of the lower thermosphere [*Fuller-Rowell*, 1995] and of thermospheric tides [*Forbes*, 1995; *Hagan*, 2000] thanks to satellite observations and numerical models.

[7] In the present paper, we will consider the daily variation as it comes from a Fourier analysis of the time series of the components of the geomagnetic field. First, we will take the data as they are, without any sorting, i.e., without discriminating between quiet days and disturbed days, or quietest days and most disturbed days, and therefore analyze *S* ("solar") variations instead of S_q variations. Then we will consider quietest days only, hereby analyzing S_q variations, in order to evaluate the influence of geomagnetic activity on the results. The Fourier analysis straightforwardly separates the various components of the daily variation. (However, only in the case of *S* is the time series continuous.) In what follows we will focus on the diurnal (24-hour) and semidiurnal (12-hour) variations, which are the most energetic *S* variations; we will not consider lunar variations.

2. Data and Analysis

[8] The observatory data used in this study are definitive hourly values obtained from the World Data Center C1 in Copenhagen. We selected 18 observatories among those having the longest series of continuously recorded hourly values for the three components: 10 midlatitude observatories distributed over several continents (Europe, Africa, Asia, North America), five high-latitude observatories and three low-latitude observatories. The name, coordinates and data series length for each selected observatory are given in Table 1. Preprocessing of data series included visual inspection and linear interpolation through gaps. Although we selected data series with as few gaps as possible, some of them have several gaps at some epochs. However, the length of those gaps is never long enough to impede the following analysis.

[9] When investigating *S* variations, data are analyzed in the following way. Let $H(t_k)$, $k = 1, \ldots, K$ a series of hourly values of the horizontal component (for example) in one of the selected observatories. Typically, K reaches up to 850,000 for the longest series of hourly values, that available at SIT. For each time t_k, the amplitudes of the 12-hour and 24-hour variations are computed over a time interval of length 28 days centered at t_k through the following formula:

$$A_T^H(k) = \left| \frac{2}{N} \sum_{n=-N/2}^{N/2} H(t_k + n\tau) \exp\left(\frac{-2i\pi n\tau}{T}\right) \right|, \qquad (1)$$

where $T = 12$ or 24 h, $\tau = 1$ h, and N is the number of points in the 28-day window.

[10] The length of the sliding window, 28 days, has been chosen so as to separate the 12-hour solar line from the geomagnetic effects of the main lunar semidiurnal tide M_2, of period about 12 h 25 min. If the window length is smaller than two weeks, the two lines are not separated by the Fourier analysis and the phenomenon of beats produces a modulation of the 12-hour line of period about 14.76 days (i.e., half a lunar month). Geomagnetic effects associated with the solar rotation (of period about 27 days) are also filtered out by this analysis.

[11] When investigating S_q variations, the analysis technique is modified as follows. Firstly, 3-hourly values are considered, starting in 1932 at the earliest, as the K_p index is only available at this frequency and after that date. Secondly, for each time t_k of the series, the five quietest 24-hour periods within the 28-day window centered at t_k are selected, according to the K_p index (retrieved from the International Service of Geomagnetic Indices). Thirdly, the amplitudes of the 12-hour and 24-hour variations are computed using

Table 1. Names, Acronyms, Coordinates, and Data Series Lengths for Observatories Used in the Study[a]

Name	Code	Geographic Latitude	Geographic Longitude	Geomagnetic Latitude	Geomagnetic Longitude	Series Length
Midlatitude, Group 1, Observatories						
Chambon-la-Forêt	CLF	48.02	2.26	43.41	79.33	1936–2002
Eskdalemuir	ESK	55.32	356.80	52.67	77.35	1914–2002
Hartland	HAD	51.00	355.52	47.59	74.79	1957–2002
Hermanus	HER	−34.43	19.23	−42.36	82.59	1941–2002
Irkutsk	IRT	52.17	104.45	47.35	177.25	1958–1990
Midlatitude, Group 2, Observatories						
Boulder	BOU	40.14	254.76	49.04	319.56	1967–2002
Honolulu	HON	21.32	202.00	21.42	269.83	1906–1975
Kakioka	KAK	36.23	140.18	29.28	211.78	1925–2002
Tucson	TUC	32.17	249.27	39.77	314.51	1910–1972
Victoria	VIC	48.52	236.58	53.80	296.04	1964–2002
High-Latitude Observatories						
Dumont d'Urville	DRV	−66.67	140.01	−80.53	235.75	1964–2002
Qeqertarsuaq	GDH	69.25	306.47	75.70	39.70	1927–1959
Meanook	MEA	54.62	246.65	62.10	305.68	1932–1975
Resolute	RES	74.69	265.11	83.34	319.57	1980–2002
Sitka	SIT	57.06	224.67	59.74	280.03	1906–2002
Low-Latitude Observatories						
Alibag	ABG	18.64	72.87	11.81	145.08	1925–1994
Bangui	BNG	4.33	18.57	−5.27	90.13	1955–2001
MBour	MBO	14.38	343.03	2.05	58.24	1953–2002

[a]The corrected geomagnetic coordinates were calculated at see level at the epoch 2000.

Equation (1), where N is the number of selected data points in the sliding 28-day window. Although Fourier analysis usually requires continuous data series, this procedure is possible because diurnal and semidiurnal variations have much larger amplitudes than day-to-day variations in geomagnetic data. However, it has an important drawback when studying semidiurnal variations: it does not completely separate the 12-hour solar line from the 12 h 25 min lunar line.

[12] In order to quantify the asymmetry between spring and fall, we introduce the following coefficient for each T line and each legal year of index j:

$$C_T^H(j) = \frac{\sum_{k\in\mathcal{F}(j)} A_T^H(k) - \sum_{k\in\mathcal{S}(j)} A_T^H(k)}{\sum_{k\in\mathcal{F}(j)\cup\mathcal{S}(j)} A_T^H(k)}\ , \qquad (2)$$

where $\mathcal{F}(j)$ is the subset of northern fall indices, referring to points between 21 June and 21 December, while $\mathcal{S}(j)$ is the subset of northern spring indices, referring to points between 1 January and 21 June and points between 21 December and 31 December. (Note that the terms "fall" and "spring" are often used to refer to the second half and first half of the year respectively rather than the usual few months surrounding the equinoxes.) It follows from this definition that $-1 \le C_T^H(j) \le 1$ for all j; if $C_T^H(j)$ is positive (resp. negative), the amplitude of the T line is larger in northern fall (resp. spring).

[13] The average seasonal variation, $\bar{A}_T^H$, is obtained by averaging A_T^H at each hour of the year over all years of the series (up to 97 years at SIT). Similarly, we compute for each observatory the mean, $\bar{C}_T^H$, and the standard deviation of the asymmetry coefficient C_T^H over all years of the series. Although the length of the data series considered is at least two solar cycles, it is not always a multiple of 11 years. Moreover, there is a significant variability of solar activity from one solar cycle to the other. For this reason, we also look at the time variations of yearly C_T^H at some observatories.

3. Results

[14] The analysis described above has been applied to the H and Z components of the field for each of the selected data series. For the purpose of results presentation, observatories have been distributed into four groups: (1) midlatitude, group 1 observatories (CLF, ESK, HAD, HER, IRT), (2) midlatitude, group 2 observatories (BOU, HON, KAK, TUC, VIC), (3) high-latitude observatories (DRV, GDH, MEA, RES, SIT), and (4) low-latitude observatories (ABG, BNG, MBO). Groups 1 and 2 include midlatitude observatories from two separate hemispheres, Europe-Africa-Asia and America-Pacific Ocean, respectively.

3.1. Average Seasonal Variation

[15] We first present results regarding the S variations, i.e., without excluding disturbed 24-hour periods from the Fourier analysis. The average seasonal variations $\bar{A}_T^H$ and $\bar{A}_T^Z$ for each T line (24 hour and 12 hour) and each group of observatories are shown on Figures 1–4.

[16] We start by describing some general features of the curves at midlatitude observatories as they come from a visual inspection of Figures 1 and 2.

[17] 1. For a given component (H or Z), the seasonal maximum of the amplitude of the 24-hour line is often larger than that of the 12-hour line. However, this is not systematical: the opposite is true for the Z component at HER and for the H component at all group 2 observatories.

[18] 2. For the Z component, the amplitude minima are generally located near the winter solstice (of the observatory hemisphere). For the H component, the situation is more complicated. For example, $\bar{A}_{24}^H$ is minimum near the summer

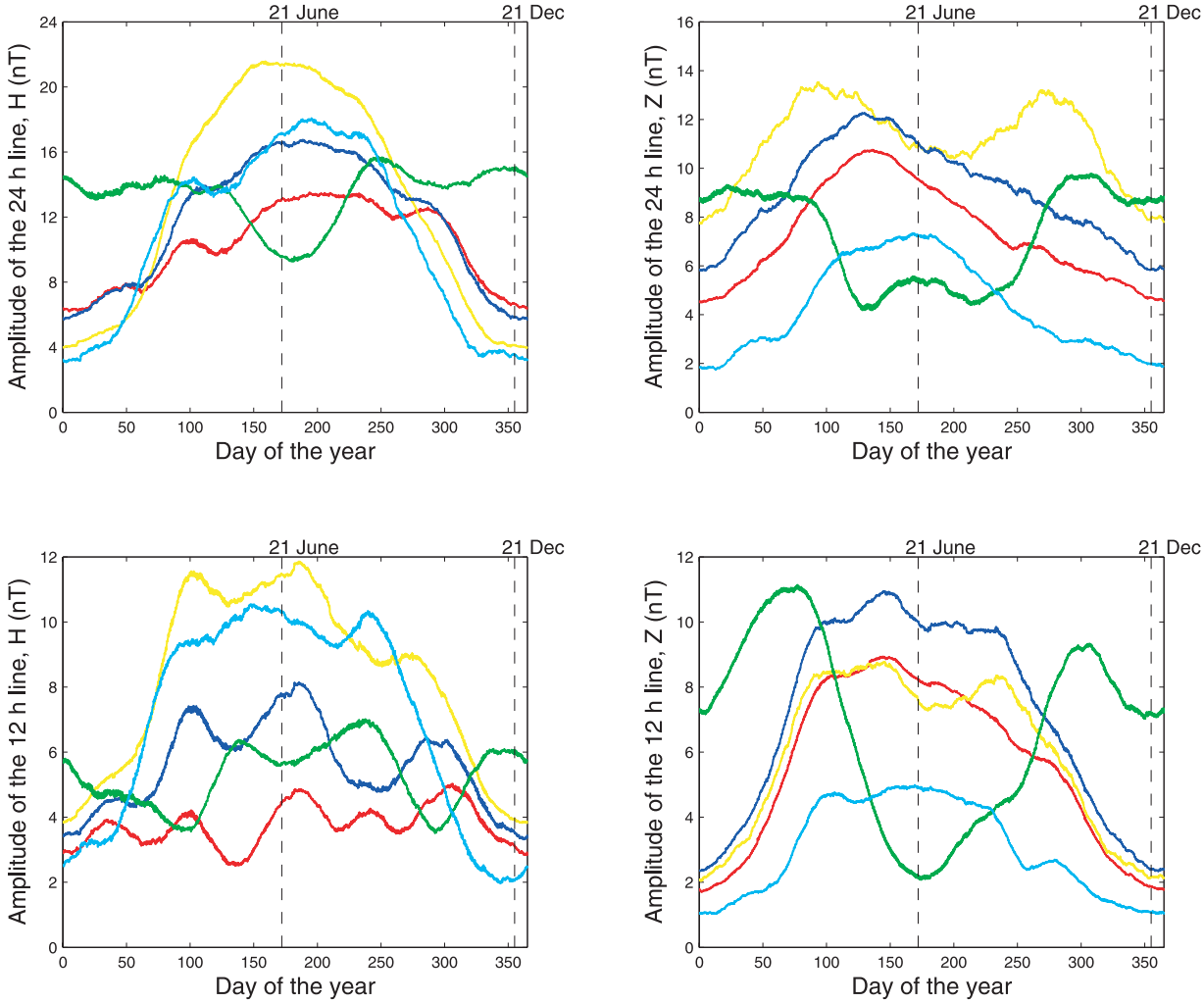

Figure 1. Average seasonal variations of the 24-hour and 12-hour line amplitudes, H and Z components, at midlatitude, group 1 observatories: CLF (red curves), ESK (yellow curves), HAD (blue curves), HER (green curves), and IRT (cyan curves).

solstice at BOU, and near the northern fall equinox at HON; $\bar{A}^H_{12}$ is minimum near the equinoxes at HER.

[19] 3. The number of maxima varies from one curve to the other. Some curves have only one maximum, located near the summer solstice (in $\bar{A}^H_{24}$ at ESK and $\bar{A}^Z_{12}$ at VIC for example) or shifted with respect to the summer solstice (in $\bar{A}^Z_{24}$ at HAD for example). Other curves have more than one maximum: two (in $\bar{A}^Z_{24}$ at ESK, $\bar{A}^Z_{12}$ at HER, and $\bar{A}^H_{12}$ at KAK for example), three (in $\bar{A}^H_{12}$ at HAD and HER), or even more (in $\bar{A}^H_{12}$ at CLF). Several curves have their two maxima near equinoxes (especially $\bar{A}^Z_{24}$ at ESK), exhibiting a clear semiannual variation. Note that the $\bar{A}^H_{12}$ curves are generally less regular than the other curves.

[20] 4. CLF and HAD curves have very similar shapes, which is not surprising as both observatories are geographically very close. Their resemblance with the IRT curves (except for A^H_{12}) is not surprising either, as all three observatories have a similar geomagnetic latitude. It is indeed well known that geomagnetic field lines strongly organize the S_q (or S) current system [*Richmond*, 1995; *Le Sager and Huang*, 2002]. Although close to HAD, ESK has a very different A^Z_{24} curve, with a clear semiannual variation, which could be related to the fact that this observatory is closer to the auroral region (see below).

[21] 5. Among group 2 observatories, BOU and VIC curves look alike due to the relatively short distance between them. TUC curves also have similar shapes, but with amplitudes generally much lower. This is not surprising as TUC is known to be near the S_q current focus [*Campbell*, 1989].

[22] As shown on Figure 3, there are important differences between curves at midlatitude observatories and those at high-latitudes observatories and also a few common features.

[23] 1. The amplitudes at high latitudes are much larger than at midlatitudes, especially those of the 24-hour line (up to 100 nT at GDH in July).

[24] 2. The amplitude of the 24-hour line is always larger than that of the 12-hour line.

[25] 3. For both components, the amplitude of the 24-hour line has a clear annual variation with a maximum near the summer solstice (of the observatory hemisphere) at all three

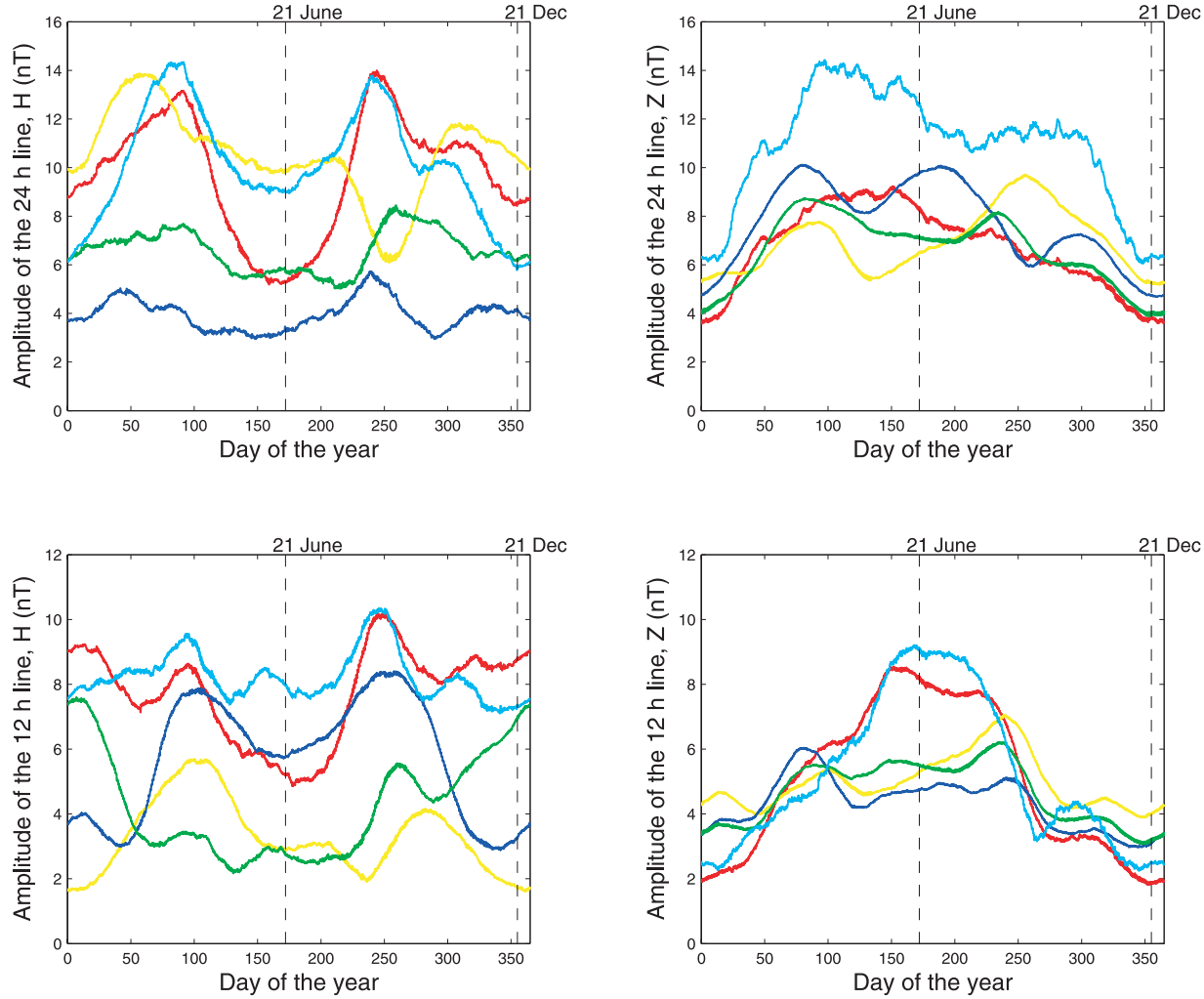

Figure 2. Average seasonal variations of the 24-hour and 12-hour line amplitudes, *H* and *Z* components, at midlatitude, group 2 observatories: BOU (red curves), HON (yellow curves), KAK (blue curves), TUC (green curves), and VIC (cyan curves).

observatories (DRV, GDH and RES) above 75° corrected geomagnetic latitude (in absolute value), a region commonly referred to as polar cap. It has a clear semiannual variation at the two observatories (MEA and SIT) between 60° and 70° corrected geomagnetic latitude (in absolute value), a region commonly referred to as auroral zone.

[26] 4. For both components, the amplitude of the 12-hour line has a strong day-to-day variability. An annual variation is clearly visible on both components at the three observatories within the polar caps (DRV, GDH and RES). However, it is not clear whether there is a semiannual variation at the two observatories within the auroral zone (MEA and SIT).

[27] 5. Because of the relatively short distance between them, GDH and RES curves have similar shapes, with more amplitude at RES on *H* for the 24-hour line and more amplitude at GDH on *Z* for both lines.

[28] Unfortunately there are very few low-latitude observatories with long, uninterrupted data series. Curves shown on Figure 4 have the following features

[29] 1. The amplitude of the 24-hour line, *H* component, is larger than at midlatitudes.

[30] 2. The amplitude of the 24-hour line is always larger than that of the 12-hour line.

[31] 3. The amplitudes for the *H* component have a clear semiannual variation at all three observatories (with the two maxima near equinoxes) and a superimposed annual variation for the 12-hour line.

[32] 4. The amplitudes for the *Z* component have more complicated variations, with one maximum near the northern fall equinox at MBO and ABG (12-hour and 24-hour lines) and one maximum near the northern spring equinox at BNG (24-hour line).

[33] 5. ABG and MBO curves have many common features, although the observatories are very far from each other. BNG curves are different; this could be related to the fact that BNG is on the other side of the geomagnetic equator, although more stations would be need to substantiate this result.

[34] Note that two effects contribute to the 12-hour geomagnetic variation: the 12-hour tide and the modulation of the currents driven by the 24-hour tide by the daily variation of ionospheric conductivity. When the second

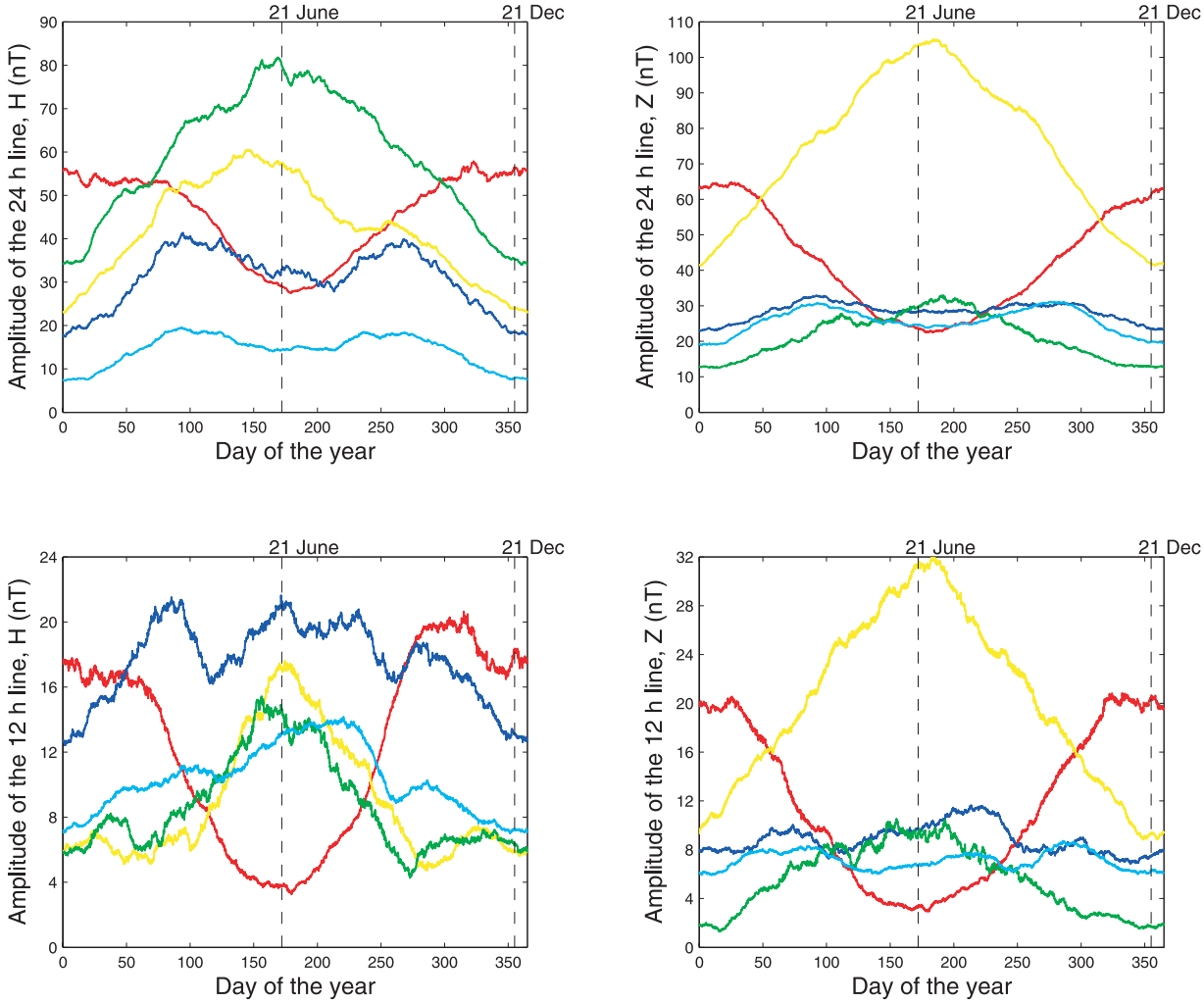

Figure 3. Average seasonal variations of the 24-hour and 12-hour line amplitudes, H and Z components, at high-latitude observatories: DRV (red curves), GDH (yellow curves), MEA (blue curves), RES (green curves), and SIT (cyan curves).

effect is dominant, the 12-hour and 24-hour lines are strongly coupled and their seasonal variations look alike (for example, the Z component at CLF, HAD, DRV, GDH and ABG). However, this is not always the case (for example, the Z component at BOU and VIC).

3.2. Average Seasonal Asymmetry

[35] Most midlatitude curves look asymmetrical about 21 June at first sight. This morphological asymmetry is conspicuous when there is only one maximum shifted with respect to the summer solstice (as in $\bar{A}^Z_{24}$ at HAD for example). In this case the amplitude has an annual variation which clearly does not follow the Sun's declination. When there is more than one maximum, the annual variation is masked by other effects which may or may not be symmetrical about 21 June; the observed asymmetry is often due to a difference between the amplitude of the spring maximum and that of the fall maximum.

[36] Once quantified by the coefficient $\bar{C}$ (Figure 5, red circles and bars), the average asymmetry between spring and fall appears to be the largest in CLF for the 24-hour line, H component, where it peaks at more than 10% (0.1) in absolute value for both the 24-hour and 12-hour lines. It is greater than 10% in absolute value for at least one line and one component in HER and HON, and greater than 5% in absolute value for at least one line and one component in 8 out of 10 observatories, the exceptions being TUC and VIC. The sign of the average asymmetry is always negative for the H component and always positive for the Z component, except in HON, where all signs are opposite to those predicted by this rule of thumb, and VIC, where only $\bar{A}^Z_{12}$ is anomalous. This observation, which is indeed conspicuous on the graphs, is remarkable as the selected observatories are widely dispersed at the Earth's surface.

[37] Compared to midlatitude curves, the high-latitude curves look somewhat more symmetrical about 21 June. The average asymmetry coefficient is indeed larger than 5% in absolute value in DRV and GDH only and does not exceed 6.9%. Unlike at midlatitudes, there is no clear relationship between the component and the sign of the asymmetry. In particular, the average asymmetries at GDH and RES generally have opposite signs although the two observatories are close to each other and the amplitude curves look similar.

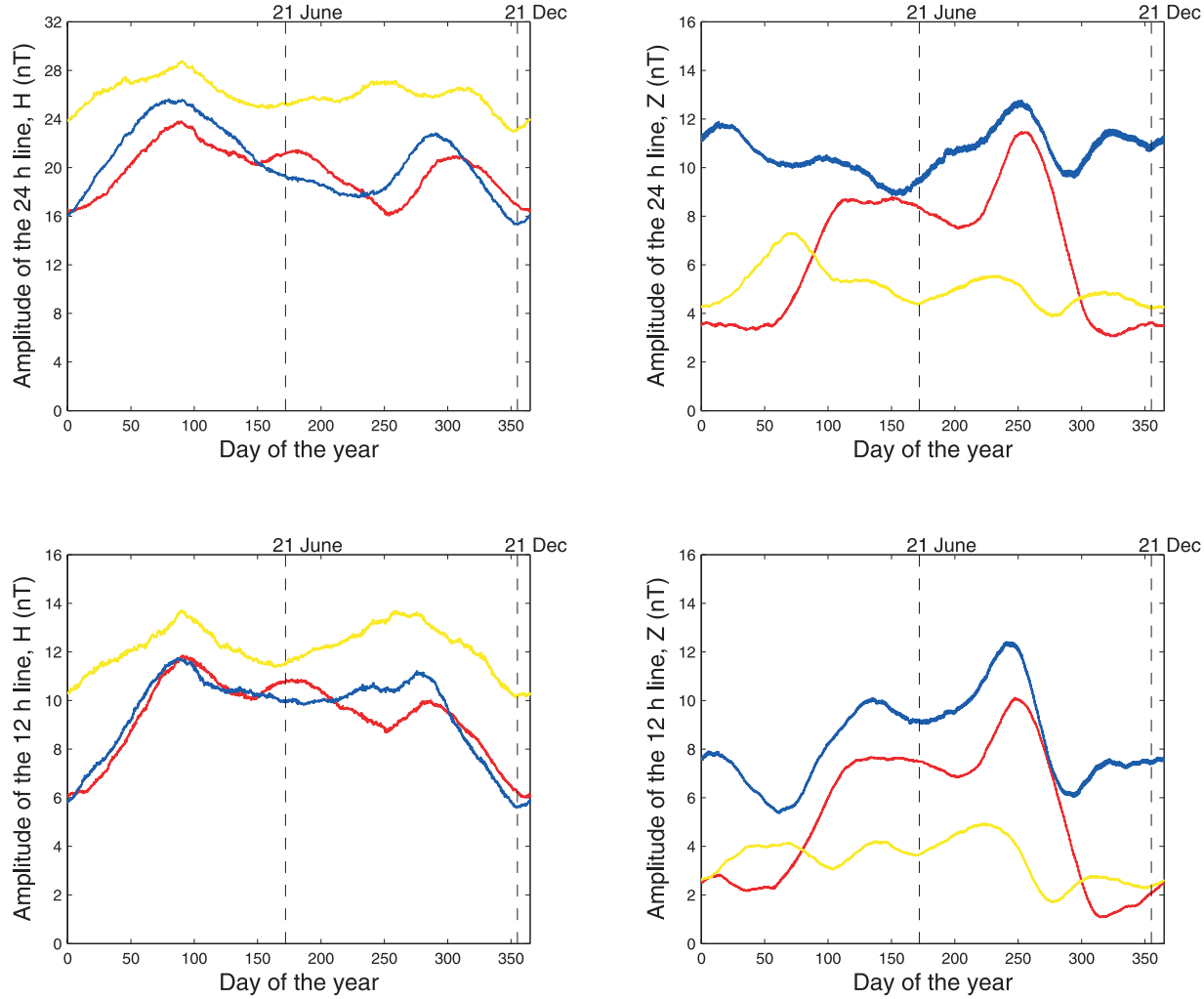

Figure 4. Average seasonal variations of the 24-hour and 12-hour line amplitudes, H and Z components, at low-latitude observatories: ABG (red curves), BNG (yellow curves), and MBO (blue curves).

[38] At low-latitude observatories, all curves look very asymmetrical for Z, less for H. This is reflected in the average asymmetry coefficient, which is largest in ABG (reaching almost 10% in absolute value) and greater than 5% in all three observatories on at least one line and one component. Like at high latitudes, there is no clear relationship here between the sign of the asymmetry and the component, except perhaps for the two observatories of the Northern magnetic hemisphere (ABG and MBO).

3.3. Time Variations of the Seasonal Asymmetry

[39] The standard deviation of the asymmetry coefficient (Figure 5, red circles and bars) is generally between 5% and 10% (0.05 and 0.1) at midlatitudes. At high latitudes the standard deviation is generally larger, both within the polar caps and the auroral zones. At low latitudes the standard deviation is comparable to that at midlatitudes.

[40] HON and all group 1 observatories have at least one line and one component such that the zero line does not lie within the standard deviation range, i.e., within the 68% confidence interval. This happens most often for the 24-hour line, H component. In CLF and HON this happens in, respectively, three and four out of the four cases considered. These results indicate that, although not in the 95% confidence interval, the asymmetry is a genuine feature of the seasonal variation at midlatitudes. (It should be stressed that the standard deviation represents the year-to-year variability of the asymmetry coefficient, not the error on the mean. This error is equal to the standard deviation divided by $\sqrt{N}$, where N is the number of years in the data series, and is therefore much smaller.)

[41] In order to investigate in more details the time variations of the seasonal asymmetry, we looked into the year-to-year variability of the seasonal asymmetry at 4 observatories among those having the longest series in Table 1: (1) CLF, the midlatitude observatory having the largest average asymmetry coefficient; (2) DRV, one of the observatories within the polar caps, where the amplitude of the 24-hour line has a dominant annual variation; (3) MEA, one of the observatories within the auroral zones, where the amplitude of the 24-hour line has a

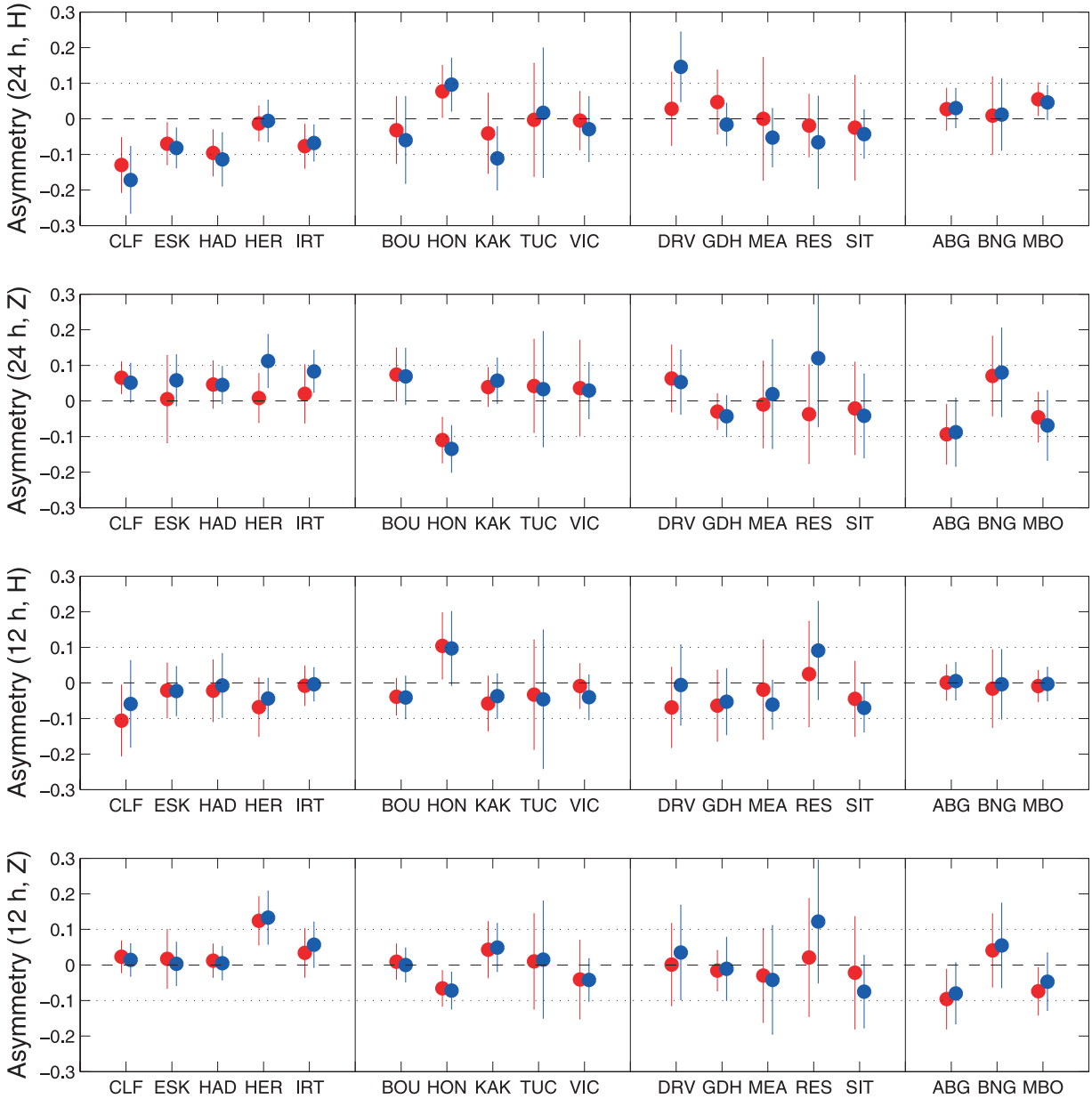

Figure 5. Means (circles) and standard deviations (bars) of the asymmetry coefficients for each line (24 and 12 hours), each component (*H* and *Z*), and each selected observatory. Coefficients are obtained either from the five quietest 24-hour periods in the sliding window (blue circles and bars) or the whole sliding window (red circles and bars).

dominant semiannual variation; and (4) MBO, one of the low-latitude observatories.

[42] Figure 6 shows the time variations of the yearly asymmetry coefficient for the 24-hour line, *H* component, at each selected observatory. Results for this line and this component are presented because the asymmetry at midlatitudes is largest in this case; results for other combinations of line and component are very similar. The following observations can be made from Figure 6.

[43] 1. The standard deviation of the asymmetry coefficient is maximum at high latitudes (DRV and MEA) and minimum at low latitudes (MBO), as already pointed out in Figure 5. At MEA and CLF, the asymmetry for a given year can be very large in absolute values: more than 0.3. Although strongly negative on average, the asymmetry at CLF can occasionally be positive; this happened four times since 1936. In fact it is easy to check this result by drawing annual curves. At CLF, the asymmetry is clearly visible on most of the curves, although quite variable.

[44] 2. There is a very strong year-to-year variability. At MEA for example, the asymmetry coefficient jumps from its minimum for the entire interval to its maximum in only one year (1943–1944). This phenomenon is observed at all four observatories, although perhaps to a lesser extent at MBO.

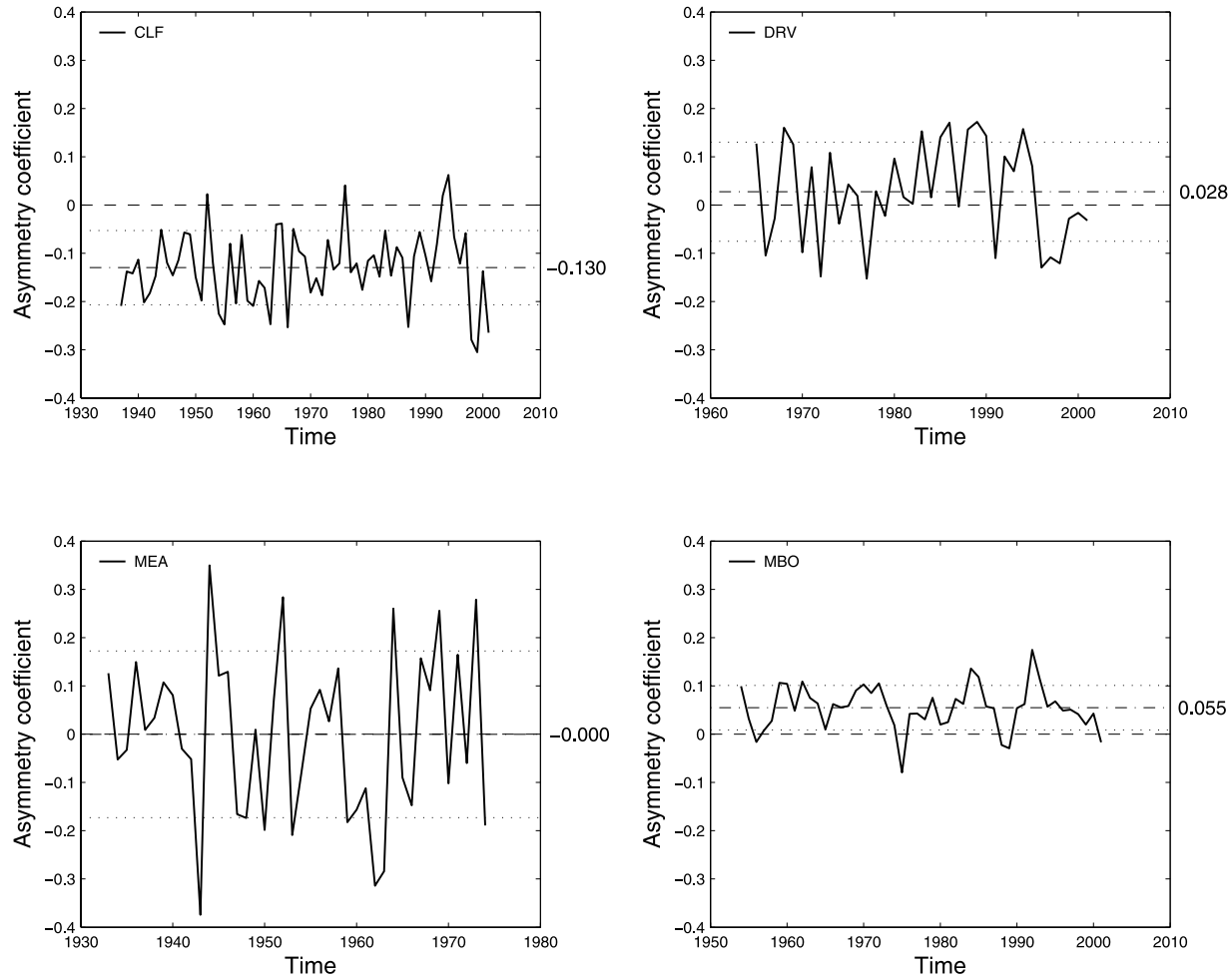

Figure 6. Time variation of the asymmetry coefficient of the 24-hour line amplitude, *H* component, at (top left) CLF, (top right) DRV, (bottom left) MEA, and (bottom right) MBO. The zero (dashed line), mean (dash-dotted line), and standard deviation range (dotted lines) are also plotted in each case.

[45] 3. Detrending and Fourier analysis confirm that there is no significant trend nor clear periodicity in all four asymmetry coefficient series. This result is all the more remarkable that it is observed at all latitudes and whatever the shape of the seasonal variation of the line amplitude, the average asymmetry and its standard deviation. Therefore we can conclude that there appears to be no correlation between the seasonal asymmetry coefficient and solar activity, as the latter has a strong variability, with both an 11-year period and a secular trend. Geomagnetic activity being strongly correlated with solar activity, this result also suggests that the seasonal asymmetry does not originate in geomagnetic activity.

3.4. Influence of Geomagnetic Activity

[46] The influence of geomagnetic activity on the seasonal asymmetry is investigated by selecting the five quietest 24-hour periods in the 28-day sliding window, as described in section 2. Figure 7 shows the average seasonal variation of the 24-hour line amplitude, *H* component, computed from the five quietest 24-hour periods in the sliding window, at the four previously selected observatories: CLF, DRV, MEA and MBO. This line, this component and these observatories have been chosen in order to illustrate the effect of geomagnetic activity on the seasonal variation. Results for other lines, components and observatories are similar, except for the 12-hour line for some components, at some observatories; however, a detailed description of this effect is beyond the scope of the present paper.

[47] It is found that geomagnetic activity increases the mean of the amplitude somewhat uniformly along the year at midlatitudes (CLF) and within the polar caps (DRV), keeping the shapes of the curves roughly unchanged. Within the auroral zones (MEA), the increase is much larger and particularly strong around equinoxes. Despite this phenomenon, the semiannual variation of the amplitude is still present in the curve computed from the quietest 24-hour periods, although less strong. At low latitudes (MBO) the effect of geomagnetic activity is small and not clear: the amplitude is a bit larger in summer when selecting quiet days, but smaller in winter.

[48] The seasonal variation of the standard deviation without data selection consists of a small annual variation

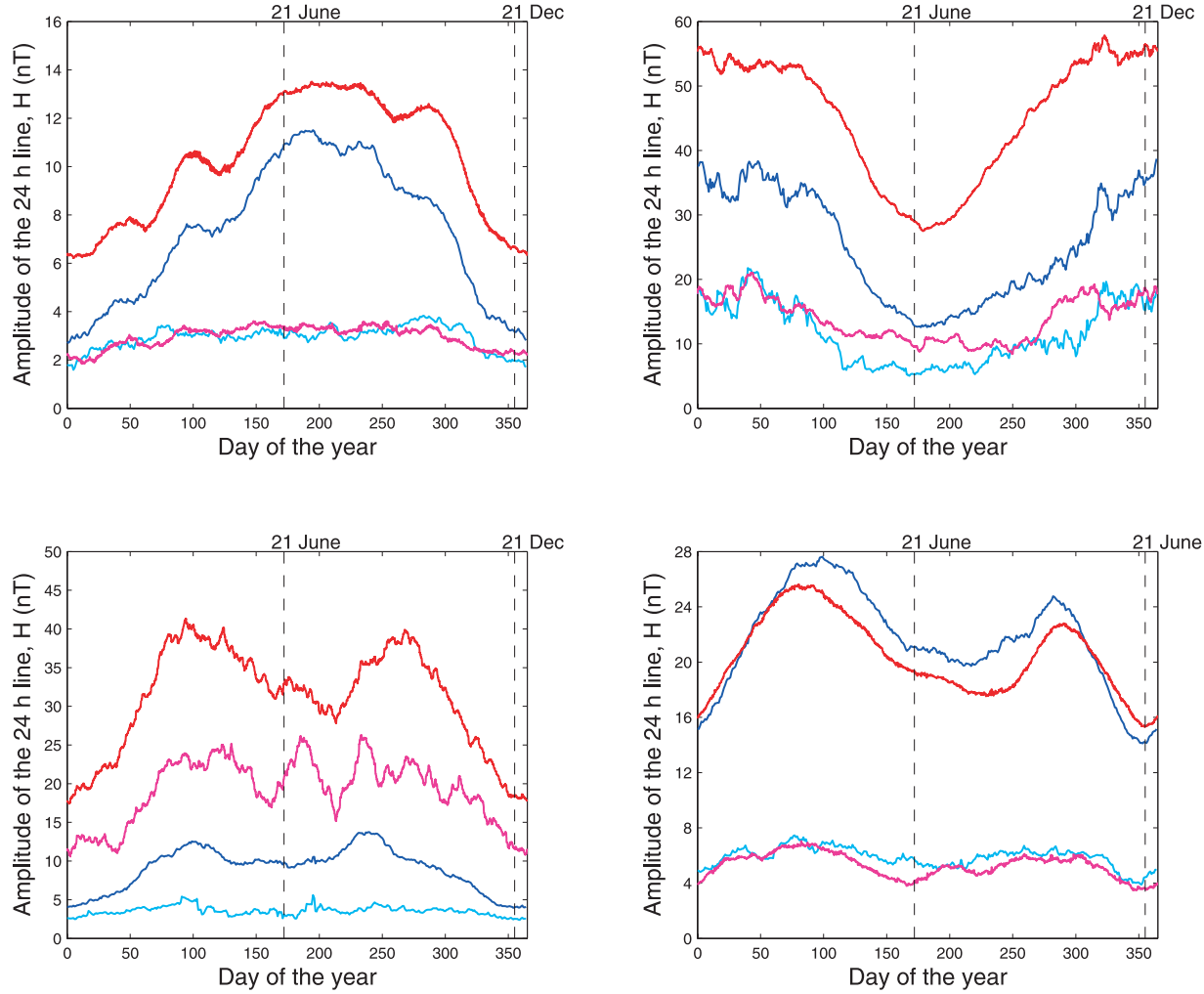

Figure 7. Means and standard deviations of the 24-hour line amplitude, *H* component, at (top left) CLF, (top right) DRV, (bottom left) MEA, and (bottom right) MBO. Red curves, means using all days; blue curves, means using the five quietest 24-hour periods; magenta curves, standard deviations using all days; cyan curves, standard deviations using the five quietest 24-hour periods.

at midlatitudes (CLF) and within the polar caps (DRV), a small semiannual variation at low latitudes (MBO) and a combination of the two in the auroral zone (MEA). The ratio of the mean to the standard deviation is minimum in the auroral zone and maximum at middle and low latitudes: it is about 5 at CLF and MBO, 3 at DRV and 2 (or even less) at MEA. The effect of geomagnetic activity on the year-to-year variability of the amplitudes is small within the polar caps and very small at middle and low latitudes. Within the auroral zones, the situation is markedly different: the standard deviation is 3 to 5 times larger when quiet days are not selected.

[49] The means and standard deviations of the asymmetry coefficients obtained when selecting the five quietest 24-hour periods are plotted in Figure 5 (blue circles and bars) for all lines, components and observatories. The following comments can be made.

[50] 1. At midlatitudes, the average asymmetry of the 24-hour lines is generally of the same sign and larger when selecting quiet days than without selection. This is most visible at CLF, BOU and KAK for the *H* component and at ESK, HER, IRT and HON for the *Z* component. At some observatories, for example ESK, the standard deviation is also smaller when selecting quiet days (but this is not always the case, see TUC for example). The effect of selecting quiet days on the 12-hour lines is not so clear: results are very similar in both cases.

[51] 2. At high latitudes the effect of selecting quiet days is similar and even stronger at several observatories: at RES, SIT and MEA, for all lines and components, at DRV for the 24-hour line, *H* component, and the 12-hour line, *Z* component. Only at GDH do the lines have a generally larger asymmetry when quiet days are not selected. The standard deviations are significantly reduced at some observatories for the 24-hour line, *H* component, but this is not a general rule.

[52] 3. At low latitudes, average asymmetries are very similar with and without selection, as well as their standard deviations.

[53] In conclusion, it is found that geomagnetic activity generally reduces the seasonal asymmetry of the diurnal and semidiurnal variations at middle and high latitudes and has no effect at low latitudes. S_q variations are thus generally more seasonally asymmetrical than S variations. Contrary to S variations, S_q variations are as asymmetrical at high latitudes as they are at midlatitudes.

4. Discussion

[54] We start by discussing our results regarding the seasonal variation of the amplitude of the 24-hour and 12-hour lines, leaving aside the results regarding the seasonal asymmetry. Those will be discussed in the following subsection.

4.1. Seasonal Variation

[55] The observed differences between S and S_q are in good agreement with theoretical predictions. Keeping all days leads to mainly two effects: (1) larger amplitudes, due to increased ionospheric conductivity and stronger atmospheric winds (due partly to Joule heating) on active days [*Richmond and Thayer*, 2000], especially at high latitudes, and (2) a larger semiannual variation of the amplitudes within the auroral zones, due to an increased activity on active days around equinoxes of active years. The second effect was observed by *Campbell and Matsushita* [1982] when comparing S_q on quiet and active years using data from North American observatories. However, contrary to these authors, we do not observe this effect at midlatitudes.

[56] At midlatitudes, the obtained amplitudes of S_q are comparable with those found in earlier studies of the S_q variations. For example, the order of magnitude of the H component cumulated amplitudes (24-hour + 12-hour) found at HON is about 20 nT, which is in good agreement with the daily variation range found by *Wulf* [1963]. A more precise comparison of our results with results from earlier studies of the S_q range would require that the amplitudes of several components not considered in this study (8-hour, 6-hour, etc.) are added to the amplitudes of the 24-hour and 12-hour lines. Moreover, it would be necessary to take into account the phases of the variations in order to add them properly.

[57] At low latitudes the large amplitude of the 24-hour line for the H component when selecting quiet days is a known feature [*Fambitakoye*, 1971; *Rastogi*, 1989]. The strong semiannual variation observed for both components at low latitudes is also a well-known effect [*Chapman and Raja Rao*, 1965; *Stening*, 1991], although not yet conclusively explained.

[58] At high latitudes the amplitudes for all components are very large when all days are considered, especially for the 24-hour line. They remain large within the polar caps even when quiet days are selected, in agreement with earlier findings by *Campbell* [1982]. This is related to the magnetospheric currents closing in the ionosphere, which are a lot larger than the S_q current system at high latitudes [*Richmond and Thayer*, 2000]. Perhaps the most striking result at high latitudes is the marked contrast between the strong annual variation within the polar caps and the strong semiannual variation within the auroral zones.

[59] Within the polar caps, the geomagnetic daily variation is principally caused by electric currents associated with the cross-polar cap electric field [*Le Sager and Svalgaard*, 2004]. This field is determined by the mapping of the interplanetary magnetic field on the ionosphere and rotates with respect to the Earth; the ionospheric conductivity in the polar caps varies with season, hence the observed annual variation. Although it varies with solar activity, a significant cross-polar electric field exists on all days. Thus this effect is also observed when selecting quiet days.

[60] There are large differences in the amplitudes of the 24-hour line at DRV, GDH and RES, and particularly in A^Z_{24} at GDH and RES while these two observatories are relatively close to each other. These differences can be attributed to two effects. First, the time span of the polar cap series are not the same and therefore the cross-polar cap electric field variations with solar activity are different. Second, the polar cap boundaries have been moving with time. For example, GDH moved from the inside of the northern polar cap in 1927 to its border in 1959 [*Le Sager and Svalgaard*, 2004]. Note that these effects could also explain the sign difference in the asymmetries at GDH and RES.

[61] To our knowledge, the semiannual variation of the 24 hour line amplitudes observed within the auroral zones has not been observed in earlier studies of S_q variations. Although the standard deviation is quite large (but recall our remark in section 3.3), the semiannual variation is clearly visible on the mean curves in Figure 7, with and without quiet days selection. It suggests that the semiannual variation of geomagnetic activity, which is enhanced in the auroral zone [*Lyatski and Tan*, 2003], affects every day the amplitude of the diurnal and semidiurnal variations within this region. Therefore auroral electrojets, which are the primary currents affected by storms and substorms, enhance the diurnal and semidiurnal variations around equinoxes, even when geomagnetic activity is low.

4.2. Seasonal Asymmetry

[62] Let us first compare our results with previous observational evidences for the seasonal asymmetry. Our results agree with those of *Wulf* [1963, 1965a] regarding the opposite signs of the seasonal asymmetry for the H component at HON and TUC. The sign of the asymmetry is probably different at HON than at TUC (and at all midlatitude observatories investigated in the present paper) because HON is on the other side of the S_q (or S) current focus. The results suggest that the focus is overhead in March at TUC (hence a lower H diurnal variation), while it is overhead in September at HON. The curves of Figure 2 also display the anomaly pointed out by *Howe* [1950]: at HON the range of the daily variation for the H component is smaller in September than in October.

[63] It is not straightforward to compare our results with those of *Campbell and Matsushita* [1982] and *Campbell and Schiffmacher* [1985] as these authors analyzed S_q variations using spherical harmonic models of equivalent ionospheric currents. They found that the external S_q current range at midlatitudes is maximal in early August over North America, in late May over Europe, and around the

summer solstice over Asia. This contradicts our result regarding the sign of the average asymmetry, which is found to be the same for a given component at all observatories considered (including American and European observatories), except HON. The reason for this discrepancy could be that *Campbell and Schiffmacher* [1985] used data from 1965 only, while we averaged the asymmetry over several decades. Such a statistical accident does not seem too improbable as the maximum current range is determined from only two or three observatories between 30° and 50° latitude in their analysis.

[64] Now let us discuss possible causes for the observed seasonal asymmetry. By far the main sources of the geomagnetic diurnal and semidiurnal variations are the lower thermospheric winds flowing in the conducting E region of the ionosphere, between 90 km and 130 km altitude. Lower thermospheric winds are known to be driven by the pressure bulge associated with the daily solar heating of the atmosphere, by diurnal and semidiurnal tides propagating upward from lower atmospheric layers, and by in situ Joule heating and ion drag by electrical currents [*Roble*, 1983; *Fuller-Rowell*, 1995]. Solar tides are mainly excited by solar radiations absorbed in the troposphere and stratosphere, and by the latent heat released from clouds in the troposphere [*Forbes*, 1995; *Hagan*, 2000]. The daily solar heating being seasonally symmetrical, the cause for the observed seasonal asymmetry is thus to be found either in geomagnetic activity or in tidal excitation and propagation.

[65] It has been clearly established in the present paper that geomagnetic activity cannot be the primary cause of the observed seasonal asymmetry. On the contrary, geomagnetic activity seems to mitigate the seasonal asymmetry: the average asymmetry coefficients at middle and high latitudes are generally larger when active days are excluded from the analysis. This effect is particularly conspicuous at high latitudes, where the effects of geomagnetic activity are the largest. It has also been demonstrated that, whatever the latitude of the observatory, the time variations of the asymmetry coefficient are independent of the solar cycle and long-term variations.

[66] Although a large amount of data pertaining to lower thermospheric winds has been collected within the past two decades, only a few observational studies have been devoted to the seasonal variability of these winds, and almost none of them places emphasis on the seasonal asymmetry. *Goncharenko and Salah* [1998] reported altitude profiles in the range 95–130 km of the semidiurnal amplitudes for different seasons, obtained using data from the Millstone Hill incoherent scatter radar collected between 1987 and 1997. Although unreported by the authors, a small seasonal asymmetry is apparent on their Figures 3 and 4, the wind amplitudes being larger in northern spring than in northern fall. A seasonal asymmetry of both the diurnal and semidiurnal tides is conspicuous on Figure 6 of *McLandress et al.* [1996], who investigated the seasonal variations of the lower thermospheric winds measured by the Wind Imaging Interferometer on the UARS satellite over a 2-year period. Using Fabry-Perot Interferometer data collected over 9 years at a high-latitude site, *Aruliah et al.* [1991] found much stronger winds at northern spring equinox than at autumn equinox around 240 km altitude.

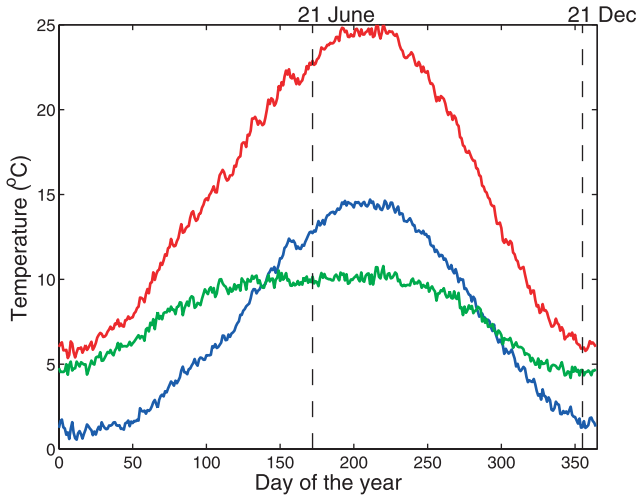

Figure 8. Average seasonal variations of the minimum temperature (blue curve), maximum temperature (red curve), and daily temperature range (green curve) recorded in Montsouris (France) from 1873 to 1998.

[67] On the theoretical side, numerical simulations of lower thermospheric winds have been generally presented at equinoxes and solar cycle minimum [*Roble and Ridley*, 1994; *Richmond*, 1995]. However, *Hagan and Forbes* [2002] recently investigated the month-to-month variations of a global-scale wave model (GSWM) in which the latent heat release was parameterized using a 7-year database of global cloud imagery. Their Figures 10 and 11 show that the seasonal variations of both the migrating and nonmigrating diurnal tides in their model are asymmetrical about the solstice at midlatitudes. Although they do not focus on the asymmetry, *Hagan and Forbes* [2002, p. 13] suggest that "the seasonal variability of the GSWM MLT migrating and nonmigrating diurnal tides is attributable to the combined effects of the mean winds that we assume in our calculations along with our forcing and dissipation parameterizations", and that nonlinear interactions between the migrating diurnal tide and planetary waves could play a role in this variability.

[68] These recent developments do not contradict the earlier proposal made by *Campbell and Matsushita* [1982] that the seasonal asymmetry observed in magnetic variations might be related to the lag between the annual cycles of temperature and insolation. We computed the average seasonal variation in a series of minimum and maximum temperatures recorded in Montsouris, Paris, over more than a century. An average seasonal asymmetry is conspicuous in Figure 8 for both the minimum and maximum temperatures; it is less obvious for the temperature range. Note that this is more than a phase shift, as the minimum occurs about a month after winter solstice, while the maximum occurs about two months after summer solstice. The time variations and the mean of the asymmetry coefficients for each of these three quantities are represented on Figure 9. The asymmetry is negative for each of these quantities. It is largest for the minimum temperature and smallest for the temperature range. Its absolute value for the minimum temperature has been slowly decreasing for more than a

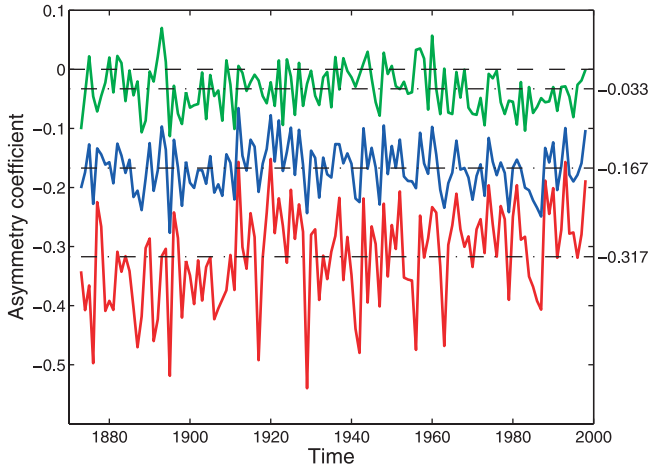

Figure 9. Time variations of the asymmetry coefficients of the minimum temperature (blue curve), maximum temperature (red curve), and daily temperature range (green curve) recorded in Montsouris (France) from 1873 to 1998. The zero (dashed line) and the means of each curve (dash-dotted lines) are also plotted.

century, which might be associated with the increase of the minimum temperature over the same period of time due to global warming (whatever its cause). Leaving aside this latter effect, the temperature curves look very similar to the magnetic curves obtained at CLF (Figures 5 and 6). However, a global investigation of this seasonal asymmetry in the temperature range is needed before we can draw conclusions regarding a possible relationship with the seasonal asymmetry observed in magnetic variations.

5. Conclusion

[69] We have investigated the seasonal variations of the amplitude of the diurnal and semidiurnal geomagnetic variations recorded at 18 observatories throughout the world, focussing on the seasonal asymmetry between spring and fall. We used hourly values of the H and Z components. For each data series, the amplitudes were computed using a 28-day window sliding over the entire length of the series (up to 97 years at SIT). One computation was performed without selecting days, the other one with selection of the five quietest 24-hour periods in the sliding window. The asymmetry between spring and fall was quantified using an ad hoc coefficient, computed for each year.

[70] Several well-known features of the seasonal variation at low latitudes and midlatitudes were reobtained, in generally good agreement with earlier studies. At high latitudes, for both lines and both components, we found a strong annual variation in the polar caps and a strong semiannual variation in the auroral zones. The former can be attributed to the annual variation of the effect of the cross-polar cap electric field and the latter to the semiannual variation of auroral electrojets. Geomagnetic activity was found to increase the amplitudes at midlatitudes and high latitudes and to increase the semiannual variation within the auroral zones.

[71] Regarding the seasonal asymmetry, four results stand out: (1) When all days are considered, the average asymmetry is maximum at midlatitudes, for both lines and both components investigated. (2) When selecting quiet days, the average asymmetry is comparable at middle and high latitudes and larger than without selecting quiet days. (3) At midlatitudes, the sign of the average asymmetry is the same in 9 out of 10 observatories for a given component, the exception being HON; it is opposite for H and Z. There is no such sign rule at high and low latitudes. (4) The time variations of the asymmetry coefficients are not correlated with solar activity.

[72] These results suggest that the seasonal asymmetry in the geomagnetic 12 h and 24 h variations at midlatitude is a global phenomenon, due to a corresponding seasonal asymmetry in the lower thermospheric winds responsible for these variations through the ionospheric dynamo. Although not systematically investigated to our knowledge, such an asymmetry is apparent in some recently published curves representing the seasonal variation of lower thermospheric winds obtained from ground and satellite data. The reasons for this asymmetry are not clear. Recent numerical simulations of diurnal and semidiurnal atmospheric tides suggest that nonlinear interactions between tides and planetary waves could be responsible for some features of the seasonal variation of these waves. The monthly temperature lag in the troposphere could also play a role. These are tentative interpretations; further observational and theoretical investigations of the seasonal asymmetry in lower thermospheric winds are needed.

[73] **Acknowledgments.** We thank Vladimir Kossobokov for useful discussions. We thank Robert Stening and an anonymous reviewer for helping to improve quite significantly the manuscript and for providing us with many relevant references. We also thank the editor for very useful suggestions. This is IPGP contribution 2054.

[74] Arthur Richmond thanks P. Le Sager and Robert Stening for their assistance in evaluating this manuscript.

References

Aruliah, A. L., D. Rees, and A. Steen (1991), Seasonal and solar cycle variations in high-latitude thermospheric winds, *Geophys. Res. Lett.*, *18*, 1983–1986.

Campbell, W. H. (1982), Annual and semiannual changes of the quiet daily variations (Sq) in the geomagnetic field at North American locations, *J. Geophys. Res.*, *87*, 785–796.

Campbell, W. H. (1989), The regular geomagnetic-field variations during quiet solar conditions, in *Geomagnetism*, edited by J. A. Jacobs, vol. 3, chap. 6, pp. 385–460, Elsevier, New York.

Campbell, W. H., and S. Matsushita (1982), Sq currents: A comparison of quiet and active year behavior, *J. Geophys. Res.*, *87*, 5305–5308.

Campbell, W. H., and E. R. Schiffmacher (1985), Quiet ionospheric currents of the Northern Hemisphere derived from geomagnetic field records, *J. Geophys. Res.*, *90*, 6475–6486. (Correction, *J. Geophys. Res.*, *91*, 9023–9024, 1986.)

Chapman, S. (1929), On the theory of the solar diurnal variation of the Earth's magnetism, *Proc. R. Soc. London, Ser. A*, *129*, 369–386.

Chapman, S., and J. Bartels (1962), *Geomagnetism*, Clarendon, Oxford, U. K.

Chapman, S., and K. S. Raja Rao (1965), The H and Z variations along and near the equatorial electrojet in India, Africa and the Pacific, *J. Atmos. Terr. Phys.*, *27*, 559–581.

Fambitakoye, O. (1971), Variabilité jour-à-jour de la variation journalière régulière du champ magnétique terrestre dans la région de l'électrojet équatorial, *C. R. Acad. Sci. Paris*, *272*, 637–640.

Forbes, J. M. (1995), Tidal and planetary waves, in *The Upper Mesosphere and Lower Thermosphere: A Review of Experiment and Theory*, *Geophys. Monogr. Ser.*, vol. 87, pp. 67–87, AGU, Washington, D. C.

Fuller-Rowell, T. J. (1995), The dynamics of the lower thermosphere, in *The Upper Mesosphere and Lower Thermosphere: A Review of Experiment and Theory*, *Geophys. Monogr. Ser.*, vol. 87, pp. 23–36, AGU, Washington, D. C.

Goncharenko, L. P., and J. E. Salah (1998), Climatology and variability of the semidiurnal tide in the lower thermosphere over Millstone Hill, *J. Geophys. Res.*, *103*, 20,715–20,726.

Gupta, J. C. (1982), Solar and lunar seasonal variations in the American sector, *Ann. Geophys.*, *38*, 255–265.

Hagan, M. E. (2000), Modeling atmospheric tidal propagation across the stratopause, in *Atmospheric Science Across the Stratopause*, *Geophys. Monogr. Ser.*, vol. 123, pp. 177–190, AGU, Washington, D. C.

Hagan, M. E., and J. M. Forbes (2002), Migrating and nonmigrating diurnal tides in the middle and upper atmosphere excited by tropospheric latent heat release, *J. Geophys. Res.*, *107*(D24), 4754, doi:10.1029/2001JD001236.

Howe, H. H. (1950), An anomaly of the magnetic daily variation at Honolulu, *J. Geophys. Res.*, *55*, 271–274.

Le Sager, P., and T. S. Huang (2002), Longitudinal dependence of the daily geomagnetic variation during quiet time, *J. Geophys. Res.*, *107*(A11), 1397, doi:10.1029/2002JA009287.

Le Sager, P., and L. Svalgaard (2004), No increase of the interplanetary electric field since 1926, *J. Geophys. Res.*, *109*, A07106, doi:10.1029/2004JA010411.

Lloyd, H. (1874), *A Treatise on Magnetism, General and Terrestrial*, Longmans Green, London.

Lyatski, W., and A. Tan (2003), Latitudinal effect in semiannual variation of geomagnetic activity, *J. Geophys. Res.*, *108*(A5), 1204, doi:10.1029/2002JA009467.

McLandress, C., G. G. Shepherd, and B. H. Solheim (1996), Satellite observations of thermospheric tides: Results from the Wind Imaging Interferometer on UARS, *J. Geophys. Res.*, *101*, 4093–4114.

Rastogi, R. G. (1989), The equatorial electrojet: Magnetic and ionospheric effects, in *Geomagnetism*, vol. 3, edited by J. A. Jacobs, chap. 7, pp. 461–525, Elsevier, New York.

Richmond, A. D. (1989), Modeling the ionosphere wind dynamo: A review, *Pure Appl. Geophys.*, *131*, 412–435.

Richmond, A. D. (1995), The ionospheric wind dynamo: Effects of its coupling with different atmospheric regions, in *The Upper Mesosphere and Lower Thermosphere: A Review of Experiment and Theory*, *Geophys. Monogr. Ser.*, vol. 87, pp. 49–65, AGU, Washington, D. C.

Richmond, A. D., and J. P. Thayer (2000), Ionospheric electrodynamics: A tutorial, in *Magnetospheric Current Systems*, *Geophys. Monogr. Ser.*, vol. 118, pp. 131–146, AGU, Washington, D. C.

Richmond, A. D., S. Matsushita, and J. D. Tarpley (1976), On the production mechanism of electric currents and fields in the ionosphere, *J. Geophys. Res.*, *81*, 547–555.

Roble, R. G. (1983), Dynamics of the Earth's thermosphere, *Rev. Geophys.*, *21*, 217–233.

Roble, R. G., and E. C. Ridley (1994), A thermosphere-ionosphere-mesosphere-electrodynamics circulation model (time-GCM): Equinox solar cycle minimum simulations (30–500 km), *Geophys. Res. Lett.*, *21*, 417–420.

Schlapp, D. M., and S. R. C. Malin (1979), Some features of the seasonal variation of the geomagnetic lunar tides, *Geophys. J. R. Astron. Soc.*, *59*, 161–170.

Stening, R. J. (1991), Variability of the equatorial electrojet: Its relations to the Sq current system and semidiurnal tides, *Geophys. Res. Lett.*, *18*, 1979–1982.

Stening, R. J., and D. E. Winch (1979), Seasonal changes in the global lunar geomagnetic variation, *J. Atmos. Terr. Phys.*, *41*, 311–323.

Takeda, M. (2002), Features of global geomagnetic S_q field from 1980 to 1990, *J. Geophys. Res.*, *107*(A9), 1252, doi:10.1029/2001JA009210.

Wulf, O. R. (1963), A possible effect of atmospheric circulation in the daily variation of the Earth's magnetic field, *Mon. Weather Rev.*, *91*, 520–526.

Wulf, O. R. (1965a), A possible effect of atmospheric circulation in the daily variation of the Earth's magnetic field, II, *Mon. Weather Rev.*, *93*, 127–132.

Wulf, O. R. (1965b), On winds in the lower ionosphere and variations of the Earth's magnetic field, *Mon. Weather Rev.*, *93*, 655–661.

E. Blanter and M. Shnirman, International Institute of Earthquake Prediction Theory and Mathematical Geophysics, Warshavskoye sh. 79 kor. 2, Moscow 113556, Russia.

A. Chulliat and J.-L. Le Mouël, Laboratoire de Géomagnétisme, Institut de Physique du Globe de Paris, 4 place Jussieu, F-75252 Paris Cedex 05, France. (chulliat@ipgp.jussieu.fr)